



## Preparation and functional analysis of gossypols having two carbohydrate appendages with enaminoxy linkages

Yoshitsugu Amano<sup>a</sup>, Masaki Nakamura<sup>a</sup>, Shinya Shiraishi<sup>b</sup>, Naoto Chigira<sup>a</sup>, Nobuya Shiozawa<sup>a</sup>, Masahito Hagio<sup>b</sup>, Tomohiro Yano<sup>c</sup>, Teruaki Hasegawa<sup>b, d, \*</sup>

<sup>a</sup> Graduate School of Life Sciences, Toyo University, 1-1-1 Izumino, Itakura-machi, Ora-gun, Gumma 374-0193, Japan

<sup>b</sup> Faculty of Life Sciences, Toyo University, 1-1-1 Izumino, Itakura-machi, Ora-gun, Gumma 374-0193, Japan

<sup>c</sup> Faculty of Food and Nutritional Sciences, 1-1-1 Izumino, Itakura-machi, Ora-gun, Gumma 374-0193, Japan

<sup>d</sup> Bio-Nano Electronics Research Centre, Toyo University, 2100 Kujirai, Kawagoe, Saitama 350-8585, Japan

### ARTICLE INFO

#### Article history:

Received 7 December 2017

Received in revised form

29 January 2018

Accepted 1 February 2018

Available online 14 February 2018

#### Keywords:

Gossypol

Glycocluster

Chemoselective coupling

Anticancer activity

Drug delivery system

### ABSTRACT

We developed new gossypol (Gos)-based glycoconjugates through dehydration condensation of native Gos and chemically modified glycosides having aminoxy groups. The resultant glycoconjugates (glycoGos) were resistant to hydrolysis, although they were light-sensitive and slowly decomposed even under indoor lighting. The glycoGos also exhibited improved water solubility compared with native Gos, but their saturated concentrations in water were still low (6.4–17  $\mu$ M), due to their hydrophobic naphthyl rings. We also carried out WST-8 assays to assess the anticancer activity of the glycoGos on DLD-1 and HepG2 cells and found that the glycoGos having  $\beta$ -lactosides and having  $\beta$ -galactosides (specific ligands for asialoglycoprotein receptors) showed enhanced anticancer activity on HepG2 cells.

© 2018 Elsevier Ltd. All rights reserved.

### 1. Introduction

Gossypol (Gos), a yellow pigment from cotton plants, exerts antioxidative [1,2], antibacterial [3], and insecticidal activities [4] and it is widely believed to play important roles in biological defense systems in these plants (Chart 1). It has also been reported that Gos has antiproliferative activity against cancer cells [5–8] and antiviral activity against influenza virus [9–11]. All of these bioactivities make Gos attractive as a research target in pharmaceutical/medicinal chemistry. However, the high cytotoxicity and low water solubility of Gos, arising from its two aldehydes and two naphthyl rings, respectively, strongly hinder its clinical applications. Many research groups have attempted to develop chemically modified Gos (Gos derivatives) with amplified bioactivity and reduced cytotoxicity [12]. A series of these works revealed that dehydration condensation between the aldehydes of Gos and various amines ( $H_2N-R$ ) is the most promising strategy to access Gos derivatives, and such Gos derivatives having imino linkages

( $-C=N-R$ ) are usually less cytotoxic than native Gos [13–15]. The advantage of dehydration condensation as a synthetic strategy relies on the following. First, it proceeds smoothly in an almost quantitative manner just by mixing the precursors (Gos and the amines). Second, neither catalyst nor additional reagent is required for the reaction. Third, no byproduct except water forms through the reaction. These points are quite advantageous for obtaining pure Gos derivatives without time/labor-consuming purification processes. Considering these advantages, a variety of Gos derivatives have been prepared. For example, Yang et al. reported dehydration condensation between Gos and various dipeptides to afford Gos–peptide conjugates and assessed their anticancer activity [16].

The introduction of carbohydrate units onto a Gos scaffold is also attractive for pharmaceutical applications, since the resultant Gos-based glycoconjugates (glycoGos) would have improved water solubility and cell specificity originating from their carbohydrate appendages. However, to date, only a couple of glycoGos have been reported in the literature [16,17].

One of these preceding works featured glycoGos having D-glucosamine appendages [16]. In this preceding paper, Gos was coupled with D-glucosamine through dehydration condensation, in which aldehydes of the former and an amino group at the C2

\* Corresponding author. Faculty of Life Sciences, Toyo University, 1-1-1 Izumino, Itakura-machi, Ora-gun, Gumma 374-0193, Japan.

E-mail address: [t-hasegawa@toyo.jp](mailto:t-hasegawa@toyo.jp) (T. Hasegawa).

position of the latter reacted with each other to give glycoGos carrying two glucosamine appendages. In this glycoGos, two aldehydes in native Gos were converted into two imino linkages and the resultant glycoGos had reduced cytotoxicity. Its enhanced anti-HIV-1 activity was also reported in this previous paper.

However, this dehydration condensation is still associated with certain problems as a general synthetic strategy to access glycoGos for pharmaceutical use, as follows. (1) Amino groups of carbohydrates are essential for the dehydration condensation and thus carbohydrates without a free amino group (e.g., glucose, galactose, mannose, *N*-acetyl-glucosamine) are not acceptable in this approach. (2) The amino group at the C2 position of D-glucosamine is usually a critical structural motif for binding with its specific lectins; therefore, the glucosamine appendages having imino groups at their C2 position should in most cases have lower affinity for these lectins. (3) In addition, the imino linkages obtained through the dehydration condensation are usually not resistant to hydrolysis (the reverse reaction of the dehydration condensation). The products would thus readily be hydrolyzed to give their precursors (Gos and the amines) under physiological conditions. The resultant Gos liberated from the Gos derivatives would have toxic effects on patients. In this respect, it is highly attractive to design glycoGos with improved water resistance.

Recently, we established an alternative synthetic approach to access glycoGos, in which chemically modified glycosides having aminoxy ( $-\text{ONH}_2$ ) groups at their C1 positions (1-*O*-aminoglycosides) were synthesized and then coupled with Gos to afford new glycoGos, in which two glycosides were attached onto a Gos scaffold with iminoxy ( $-\text{C}=\text{N}-\text{O}-\text{R}$ ) linkages. It is widely recognized by organic chemists that aminoxy groups react with aldehydes in a chemoselective manner to form iminoxy linkages that are robust even in aqueous media [18–21]. Furthermore, these new glycoGos have *O*-linked glycosides and thus the carbohydrate units should retain their inherent affinities towards their specific lectins. We herein report synthetic procedures to access our new glycoGos, their solubility, and their anticancer activity.

## 2. Results and discussion

### 2.1. Synthesis of 1-*O*-aminoglycosides

The 1-*O*-aminoglycosides were obtained through synthetic

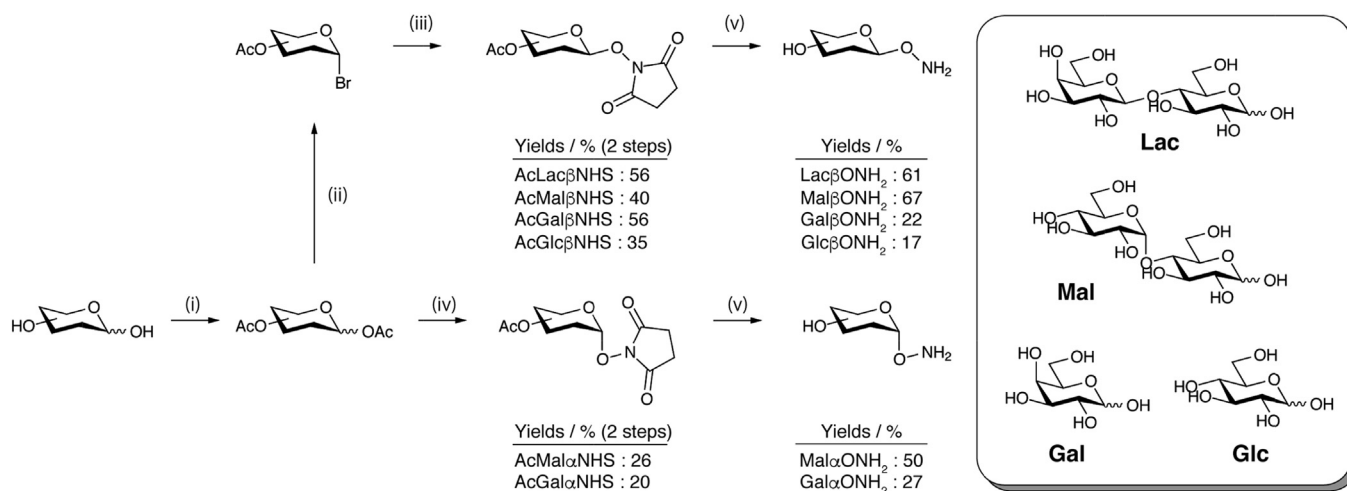
routes reported in the literature (Scheme 1) [22]. In the case of lactose (Lac), for example, commercially available Lac monohydrate was acetylated with acetic anhydride and pyridine, and the resultant *per*-acetylated lactose (AcLac) was then brominated with HBr [23]. The resultant lactosyl bromide (AcLacBr) was glycosylated with *N*-hydroxysuccinimide (NHS) in a biphasic solvent system containing  $\text{Na}_2\text{CO}_3$  and tetrabutylammonium hydrogen sulfate (TBAHS) to afford *per*-acetylated lactoside having  $\beta$ -linked NHS aglycon (AcLac $\beta$ NHS) at a 56% yield (two steps from AcLac). The other  $\beta$ -linked NHS-glycosides (AcMal $\beta$ NHS, AcGal $\beta$ NHS, and AcGlc $\beta$ NHS) were also obtained through similar synthetic procedures at moderate yields (40%, 56%, and 35%, respectively).

On the other hand, the corresponding glycosides having  $\alpha$ -linked NHS aglycons were prepared through alternative routes. For example, in the case of maltose (Mal), AcMal was subjected to glycosylation with NHS in the presence of  $\text{BF}_3\text{OEt}_2$  to give *per*-acetylated Mal having  $\alpha$ -linked NHS aglycon (AcMal $\alpha$ NHS). In this reaction, the product was a mixture containing AcMal $\alpha$ NHS (major product) and AcMal $\beta$ NHS (minor product). We carried out repeated column purification processes using various solvent systems and finally retrieved AcMal $\alpha$ NHS in its pure form. This purification process greatly deteriorated the yield of this glycosylation step. *Per*-acetylated galactoside having  $\alpha$ -linked NHS aglycon (AcGal $\alpha$ NHS) was also obtained through a similar reaction scheme starting from galactose.

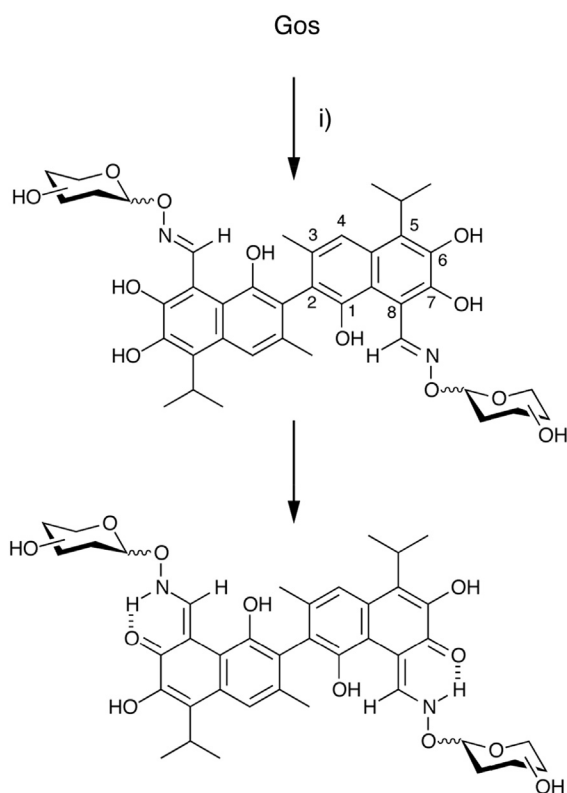
With these six  $\alpha/\beta$ -linked NHS-glycosides in hand, we carried out simultaneous removal of the *O*-acetyl and *N,N*-succinimidyl groups from these NHS-glycosides by treating them with hydrazine monohydrate to give the corresponding 1-*O*-aminoglycosides.

### 2.2. Coupling between Gos and 1-*O*-aminoglycosides

The dehydration condensation of Gos with the 1-*O*-aminoglycosides was achieved by mixing the former (1 eq.) and excess amounts of the latter (3 eq.) in dry MeOH and evaporation of the resultant mixtures (Scheme 2). Removal of the unreacted 1-*O*-aminoglycosides from the residue was achieved by washing them with small amounts of cold water to obtain the glycoGos in their pure forms. Successful syntheses of the desired glycoGos were confirmed through electrospray ionization time-of-flight mass (ESI-TOF-MS) spectral measurements. For example, in the case of the dehydration condensation of Gos with 1-*O*-amino- $\beta$ -lactoside



**Scheme 1.** Synthesis of 1-*O*-aminoglycosides: i)  $\text{Ac}_2\text{O}$ , Py, rt, 17–43 h, ii) HBr, acetic acid,  $\text{Ac}_2\text{O}$ ,  $\text{CH}_2\text{Cl}_2$ , rt, 1.5–2.0 h, iii) NHS, TBAHS,  $\text{CH}_2\text{Cl}_2$ ,  $\text{Na}_2\text{CO}_3$  aq, rt, 8.5–13 h, iv) NHS,  $\text{BF}_3\text{OEt}_2$ ,  $\text{CH}_2\text{Cl}_2$ , under  $\text{N}_2$ , rt, 22–24 h, v) hydrazine monohydrate, dry MeOH, rt, 2–5 h (see Experimental for the detailed reaction time and yield of each carbohydrate derivative).



**Scheme 2.** Dehydration condensation of Gos and the 1-*O*-aminoglycosides followed by the structural rearrangement to afford glycoGos having two enaminoxy linkages (See [Scheme 1](#) for the detailed carbohydrate structures): i) the 1-*O*-aminoglycosides (3 eq. for Gos), in dry MeOH, rt, 4–5 h.

(Lac $\beta$ ONH<sub>2</sub>), the ESI-TOF-MS spectrum of the product showed a molecular ion peak (*m/z*) at 1197.4374, which was attributed to Gos having two  $\beta$ -lactoside appendages ( $\beta$ Lac<sub>2</sub>Gos, calc. = 1197.4350 for C<sub>54</sub>H<sub>72</sub>N<sub>2</sub>O<sub>28</sub>+H), proving its successful synthesis. Other glycoGos also showed their molecular ion peaks at *m/z* values expected from their elemental compositions.

In addition to the ESI-TOF-MS spectra, <sup>1</sup>H NMR spectra of the products also showed clear evidence of the quantitative conversion from Gos to glycoGos. For example, native Gos showed two singlet <sup>1</sup>H NMR peaks at 10.68 and 10.66 ppm ([Fig. 1-a](#)). These two peaks should stem from some of the aldehyde-related structures (*cis/trans*-aldehydes, hemiacetals, or enols; see [Scheme S1](#)) of Gos. In contrast,  $\beta$ Lac<sub>2</sub>Gos obtained through our synthetic procedure showed no peak around 10.6 ppm, indicating that the aldehydes were quantitatively converted into the iminoxy linkages through the reaction ([Fig. 1-b](#)).

### 2.3. Structural details of glycoGos

As we mentioned above, our glycoGos showed no aldehyde-derived peak in their <sup>1</sup>H NMR spectra, clearly showing that both of the two aldehydes in native Gos quantitatively reacted with the 1-*O*-aminoglycosides. In addition, we also found that a broad peak (14.1 ppm) of native Gos attributable to its C7OH also disappeared through the reaction and two singlet peaks derived from enaminoxy (C8=CH-NHO-) linkages newly appeared at around 10.0 and 11.7 ppm. This spectral feature shows that structural rearrangements occurred and the iminoxy linkages first formed through the dehydration condensation were thereafter converted into enaminoxy ones ([Scheme 2](#), bottom). Similar structural rearrangements

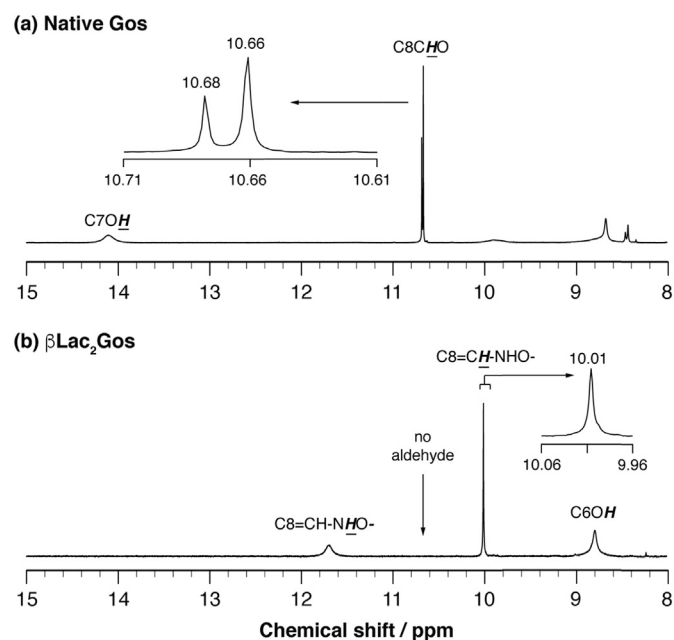


**Fig. 1.** Partial <sup>1</sup>H NMR spectra (15–8 ppm) of native Gos (a) and  $\beta$ Lac<sub>2</sub>Gos (b) in DMF-*d*<sub>7</sub> (300 MHz, rt). See [supplementary information](#) for their whole spectra.

were also reported in the literature, although the linker structures were enamine linkages in these previous works.

The glycoGos having enaminoxy linkages were also supported by molecular dynamics (MD) calculations on  $\alpha$ Mal<sub>2</sub>Gos as a representative. In these calculation processes, we built three  $\alpha$ Mal<sub>2</sub>Gos models in which the linkages between the Gos scaffold and the carbohydrate appendages were different from each other; that is, one model had two iminoxy linkages ( $\alpha$ Mal<sub>2</sub>Gos<sub>ii</sub>), another had enaminoxy and iminoxy ones ( $\alpha$ Mal<sub>2</sub>Gos<sub>ei</sub>), and the other had two enaminoxy ones ( $\alpha$ Mal<sub>2</sub>Gos<sub>ee</sub>) ([Chart S1](#)). We then carried out MD calculations (Discovery Studio 4.5, CHARMM, 300 K,  $\epsilon$  = 80, 10 ns equilibration, 90 ns dynamics) on these three models, revealing that their average potential energies during the dynamics were 221.7  $\pm$  5.8 ( $\alpha$ Mal<sub>2</sub>Gos<sub>ii</sub>), 219.1  $\pm$  7.2 ( $\alpha$ Mal<sub>2</sub>Gos<sub>ei</sub>), and 211.0  $\pm$  6.1 kcal/mol ( $\alpha$ Mal<sub>2</sub>Gos<sub>ee</sub>) ([Fig. S1](#)). These data clearly indicate that  $\alpha$ Mal<sub>2</sub>Gos having two enaminoxy linkages ( $\alpha$ Mal<sub>2</sub>Gos<sub>ee</sub>) is the most stable isomer.

### 2.4. UV-vis spectra of glycoGos

Native Gos showed a broad absorption peak at 378 nm in its UV-vis spectrum ([Fig. 2-a](#)). On the other hand, each glycoGos showed a peak at around 355 nm that was blue-shifted (ca. 23 nm) from that of native Gos. In addition, their intensities were amplified by factors of 1.05–1.25 compared with that of native Gos.

Interestingly, the UV-vis spectra of the glycoGos changed in a concentration-dependent manner. In the case of  $\beta$ Lac<sub>2</sub>Gos, for example, it showed a strong absorption peak at 356 nm with its molar extinction coefficient ( $\epsilon$ ) of  $1.8 \times 10^4$  M<sup>-1</sup>cm<sup>-1</sup> when [ $\beta$ Lac<sub>2</sub>Gos] was 1000  $\mu$ M (in DMF, [Fig. 2-b](#)). In contrast, its  $\epsilon$  value became small upon dilution and that of a shoulder peak (430 nm) was simultaneously amplified. We carried out the following experiments to confirm that the hydrolysis of glycoGos is not responsible for the concentration-dependent UV-vis spectral change. (1) Even when we used carefully dried DMF and wet DMF, similar concentration-dependent UV-vis spectral changes were observed for both of these glycoGos solutions. This finding showed that water molecules in the DMF solutions have no critical effect on

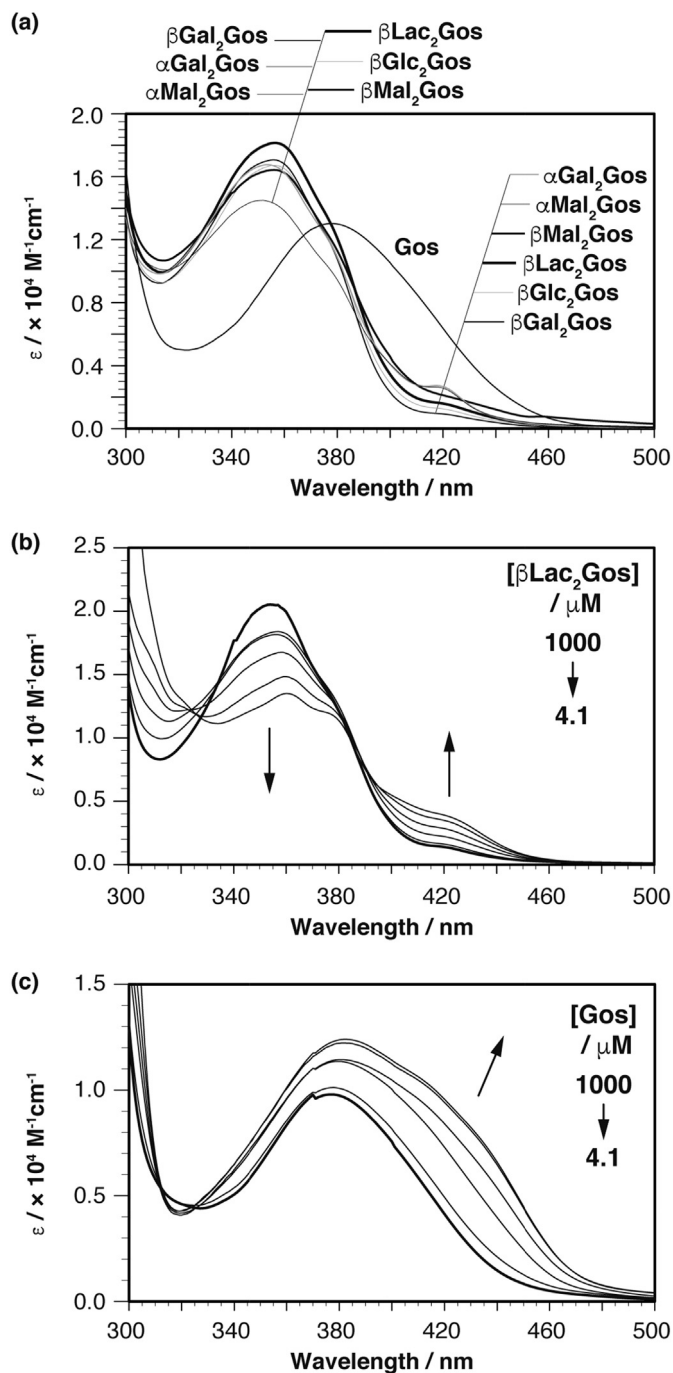


**Fig. 2.** UV-vis spectra of glycoGos and Gos ([glycoGos] or [Gos] = 1 mM) (a) and concentration-dependent UV-vis spectral changes of  $\beta$ Lac<sub>2</sub>Gos (b) and Gos (c): in DMF, rt. (See SI for colored version of Fig. 2-a).

the concentration-dependent UV-vis spectral change. (2) No peak attributable to Gos or Lac $\beta$ ONH<sub>2</sub>, which are hydrolysis products liberated from  $\beta$ Lac<sub>2</sub>Gos, was observed through the ESI-TOF-MS spectral analysis. (3) Native Gos also showed concentration-dependent UV-vis spectral change in its DMF solution (Fig. 2-c). Taking these findings together, we rule out the possibility of the hydrolysis of the enaminooxy linkages being the mechanism behind these concentration-dependent UV-vis spectral changes. Instead, we assume that molecular-level aggregation of the glycoGos contributes to the concentration-dependent spectral changes. Note that these concentration-dependent UV-vis spectral changes

have a clear isosbestic point at around 382 nm. Since the  $\epsilon$  value of this isosbestic point is not affected by the glycoGos concentrations, the absorbance at this wavelength is quite useful to assess the concentrations of glycoGos solutions in a quantitative manner (see the next section for details).

### 2.5. Water solubility of glycoGos

The introduction of carbohydrate units is one of the most widely accepted strategies to improve the water solubility of organic/inorganic compounds. This was also the case for Gos; that is, glycoGos showed enhanced water solubility in comparison to native Gos. To assess their water solubility, we put native Gos and the glycoGos into limited amounts of water and incubated the resultant suspensions at ambient temperature for ca. 10 min. In the case of native Gos, the supernatant of the resultant suspension was colorless, confirming that it was hardly water-soluble. However, the supernatants obtained from the glycoGos were pale yellow, suggesting their improved solubility. We then estimated the saturated concentrations of the glycoGos in water via the following procedure. Briefly, we mixed a small aliquot of the supernatant obtained from each of the aqueous glycoGos suspensions with DMF (final DMF/water ratio = 90:10 v/v). We then estimated the glycoGos concentration of the original supernatant based on absorbance at the isosbestic point (382 nm) of these DMF-rich solutions (Table 1). The saturated concentration of native Gos in water is lower than 0.1  $\mu$ M, which was too low to be quantified. The sub-micromolar solubility of native Gos has also been reported in the literature [24]. In contrast, the saturated concentrations of our glycoGos were in the range of 6.4–17  $\mu$ M.

### 2.6. Photo-stability of glycoGos in solution

We designed our glycoGos to have improved resistance to hydrolysis. In fact, all of our experimental data, especially the ESI-TOF-MS spectra, showed that our glycoGos are resistant to hydrolysis and they do not give rise to their precursors even if stored in aqueous media. However, it should be noted that our glycoGos are light-sensitive and gradually decompose into various impurities in few days, even under indoor lighting. For example, in the first stage of our study, we attempted to purify the glycoGos obtained from the dehydration condensation through size-exclusion chromatography (TOYOPEARL HW40S, TOSOH) using methanol as an eluent. The glycoGos were almost pure before the column chromatographic process, but the compounds eluted out from the column were mixtures of various impurities. The TLC analysis showed that the impurities were neither Gos nor the 1-O-aminoglycosides, suggesting that hydrolysis of the glycoGos is not responsible for their decomposition. Note that this chromatographic process was carried out under indoor lighting and it took 2–3 days until the compounds were eluted out. It should also be noted that the glycoGos were also decomposed when we stored their solutions in flasks without the size-exclusion gel. We assume that the glycoGos are light-sensitive and they were slowly decomposed even under

**Table 1**

Solubility of the glycoGos and native Gos in water.

	Saturated concentration/ $\mu$ M
$\beta$ Lac <sub>2</sub> Gos	6.4
$\beta$ Gal <sub>2</sub> Gos	7.3
$\beta$ Mal <sub>2</sub> Gos	8.5
$\alpha$ Mal <sub>2</sub> Gos	17
Gos	<0.1 <sup>a</sup>

<sup>a</sup> Too low to be quantified.

indoor lighting, although chemical structures of the products resulting from the light-induced decomposition have not yet been clarified.

The light-induced decomposition of the glycoGos was clearly supported by their limited UV-vis spectral change without indoor lighting. In detail, we prepared two DMF solutions containing the glycoGos and kept each of them under indoor lighting or in the dark to measure their UV-vis spectra every 1 h. Through this experiment, we found that the absorption peak at 354 nm that is characteristic of the glycoGos was gradually weakened under the lighting and after 24 h it reached a level 83% of that of freshly prepared solution (Fig. 3). In contrast, the other sample kept in the dark still had 91% intensity of this absorption peak in comparison to the original one. Note that the slight weakening of intensity (9%) of the latter sample should have arisen from photo-induced decomposition via unavoidable indoor light irradiation during sample manipulation. Oxidative decomposition with  $O_2$  in the medium was also conceivable as one of the mechanisms behind the UV-vis spectral change.

### 2.7. Anticancer activity of glycoGos

Anticancer activity of glycoGos was assessed on colorectal adenocarcinoma (DLD-1) and hepatocellular carcinoma (HepG2) cells. Briefly, these cells were treated with increasing doses of the glycoGos for 48 h and then viable cell numbers were assessed through WST-8 assays, which revealed that they showed unique anticancer activities that were clearly different from those of native Gos. In detail, in the case of native Gos, the viable cell numbers monotonically decreased in a dose-dependent manner, with  $IC_{50}$  values of 13 and 17  $\mu M$  for DLD-1 and HepG2 cells, respectively (Fig. 4). Such strong anticancer activity should in part stem from the highly cytotoxic aldehyde groups of native Gos. Note that these data on native Gos showed that it had lower anticancer activity on HepG2 than on DLD-1.

On the other hand, some glycoGos showed unique anticancer activities that were clearly different from those of native Gos. For

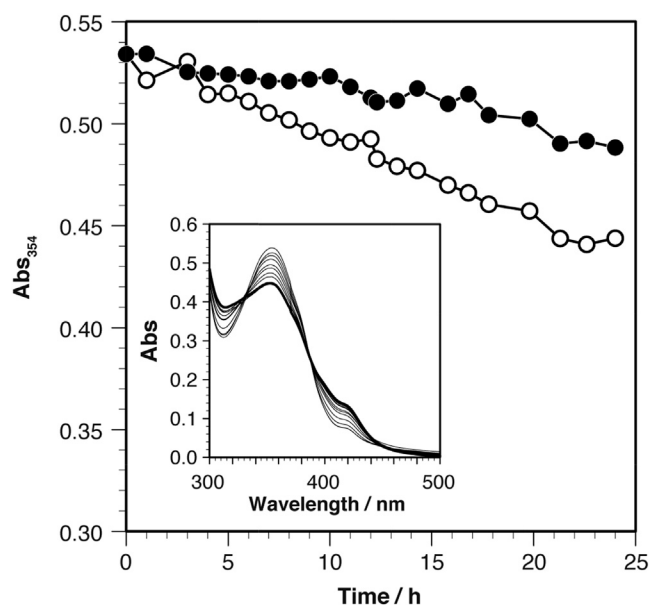


**Fig. 3.** UV-vis spectral change of  $\alpha Mal_2 Gos$  solution under the indoor lighting (inset) and time-courses of the UV-vis spectral changes of  $\alpha Mal_2 Gos$  solution under the indoor lighting (open circle) and in the dark (closed circle); [ $\alpha Mal_2 Gos$ ] = 270  $\mu M$ , in DMF, rt,  $\lambda = 1$  mm.

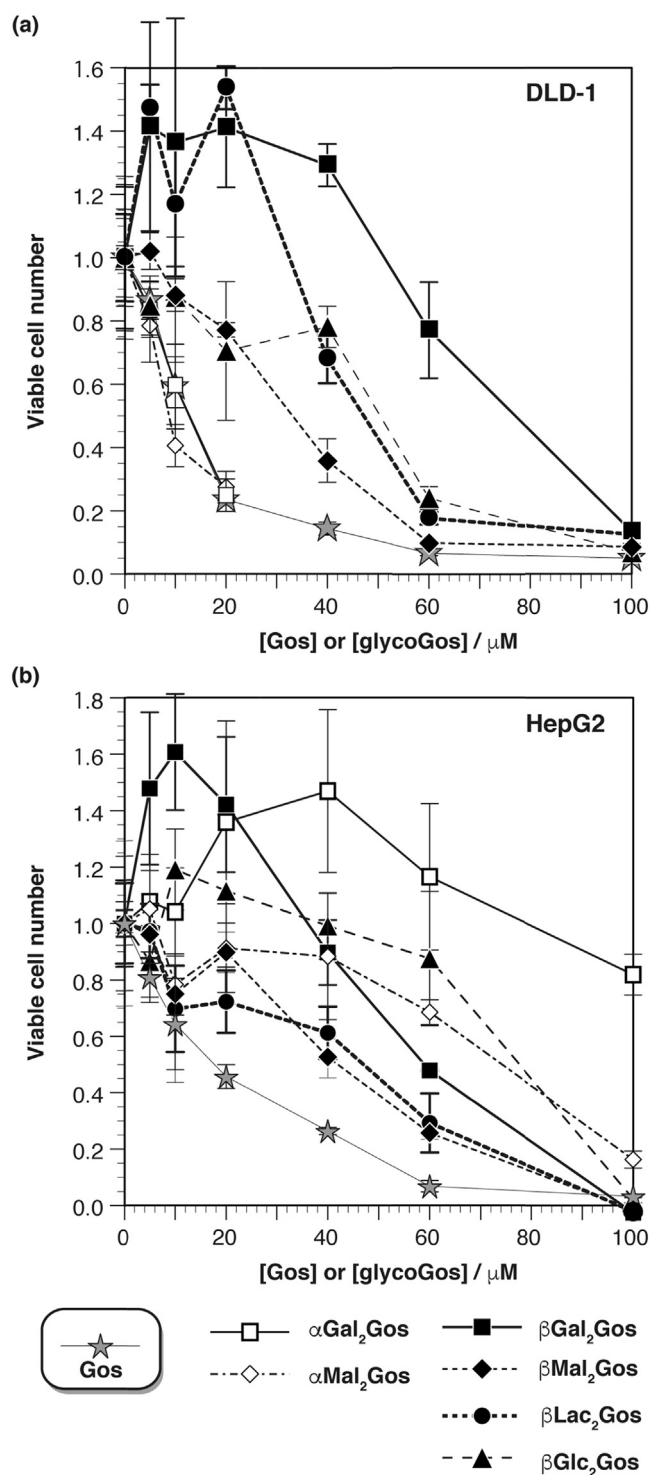


**Fig. 4.** Viable cell numbers of DLD-1 (a) and HepG2 (b) after the treatment with Gos or glycoGos.

example, in the case of  $\beta Gal_2 Gos$ , the viable cell numbers of both DLD-1 and HepG2 increased in a dose-dependent manner until the doses reached ca. 10–40  $\mu M$ ; then, they conversely decreased in a dose-dependent manner.  $\beta Lac_2 Gos$  and  $\beta Gal_2 Gos$  also showed similar anticancer activities for DLD-1 and HepG2 cells, respectively. Although we have no information to reasonably explain the mechanisms of these unique anticancer activities, the fact that only certain combinations of the glycoGos and the cells showed unique

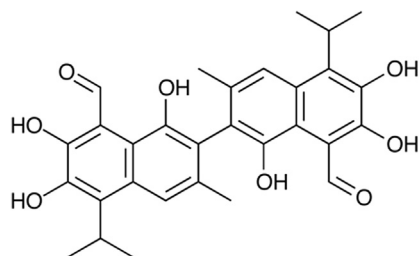


Chart 1. Structure of Gos.

anticancer activities suggests that the carbohydrate appendages play substantial roles in their anticancer activities.

We estimated the  $IC_{50}$  values of the glycoGos on these cells based on their anticancer activities, revealing that most glycoGos showed higher  $IC_{50}$  (lower anticancer activities) on these cells than those obtained by native Gos (Table 2). Specifically, in the case of HepG2, all glycoGos showed higher  $IC_{50}$  than that obtained for native Gos ( $IC_{50} = 17 \mu\text{M}$ ). This was also largely true for DLD-1. In this case, although certain glycoGos ( $\alpha\text{Gal}_2\text{Gos}$  and  $\alpha\text{Mal}_2\text{Gos}$ ) showed  $IC_{50}$  values that were equal to or lower than that obtained by native Gos ( $13 \mu\text{M}$ ), most glycoGos showed higher ones. We assume that chemical conversion of the highly cytotoxic aldehydes into enaminoxy linkages was responsible for the lower anticancer activities of the glycoGos.

Most glycoGos ( $\alpha\text{Gal}_2\text{Gos}$ ,  $\beta\text{Mal}_2\text{Gos}$ ,  $\alpha\text{Mal}_2\text{Gos}$ , and  $\beta\text{Glc}_2\text{Gos}$ ) showed a higher  $IC_{50}$  for HepG2 than for DLD-1. The exceptions were  $\beta\text{Lac}_2\text{Gos}$  and  $\beta\text{Gal}_2\text{Gos}$ , which showed similar or lower  $IC_{50}$  for HepG2 than for DLD-1. These findings showed that the introduction of  $\beta\text{Lac}$  or  $\beta\text{Gal}$  units onto the Gos scaffold enhances its anticancer activity against HepG2 in a cell-specific manner. Asialoglycoprotein receptors (AGPR) that are specifically expressed on HepG2 cell surfaces should bind the carbohydrate appendages of  $\beta\text{Lac}_2\text{Gos}$  and  $\beta\text{Gal}_2\text{Gos}$  to increase their cellular uptake.

Finally, we observed the DLD-1 and HepG2 cells under an optical microscope after their treatment with the glycoGos or native Gos. We clearly observed apoptotic bodies for these cells, showing that not only native Gos but also the glycoGos induce their apoptosis and that such enhancement of apoptosis is responsible for their anticancer activities (Fig. S3). The enhanced apoptosis induced by native Gos and the Gos derivatives has also been reported in the literature [25].

### 3. Conclusion

We synthesized bis-glycosylated Gos through the dehydration condensation between native Gos and 1-O-aminoglycosides. The resultant glycoGos were resistant to hydrolysis but readily decomposed in few days under indoor lighting. Although the glycoGos had improved water solubility in comparison to native Gos,

their water solubility was still limited ( $6.4\text{--}17 \mu\text{M}$ ). The glycoGos ( $\beta\text{Lac}_2\text{Gos}$  and  $\beta\text{Gal}_2\text{Gos}$ ) carrying specific carbohydrate ligands for AGPR showed enhanced anticancer activities on HepG2 cells, although their cell specificities were still limited. These findings clearly show that the introduction of two carbohydrate units is not sufficient to develop glycoGos with excellent water solubility and cell specificity. We are now focusing our synthetic efforts on developing dendritic compounds having Gos cores and more than eight carbohydrate appendages. We expect that such dendritic compounds should have excellent properties as potential water-soluble/cell-specific anticancer drugs.

## 4. Experimental

### 4.1. General

$^1\text{H}$  and  $^{13}\text{C}$  NMR spectra were acquired on a JEOL AL300 (JEOL Resonance, Ltd) in  $\text{CDCl}_3$ ,  $\text{CD}_3\text{OD}$ ,  $\text{D}_2\text{O}$  or  $\text{DMF-}d_7$ . The chemical shifts were reported in ppm ( $\delta$ ) relative to  $\text{Me}_4\text{Si}$  or internal references such as HOD. IR spectra were recorded on an FT/IR-4100 Fourier transform infrared spectrometer (JASCO Co., Ltd). Matrix assisted laser desorption ionization time-of-flight (MALDI-TOF) mass spectra were recorded on AXIMA-CFR+ (SHIMADZU, Ltd) or AXIMA-Confidence (SHIMADZU, Ltd). High-resolution electrospray ionization time-of-flight (HR-ESI-TOF) mass spectra were recorded on SYNAPT G2 HDMS (Waters, Co.). UV-vis spectra were recorded on a JASCO V-630 Spectrophotometer (JASCO Co., Ltd). Molecular dynamics calculations were carried out on Discovery Studio 4.5 (Dassault systems). Observations of DLD-1 and HepG2 cells were carried out using Primo Vert (Zeiss). Silica gel 60 N (spherical, neutral, particle size  $63\text{--}210 \mu\text{m}$ ) for column chromatography was purchased from Kanto Chemical Co., INC. Thin layer chromatography (TLC) was carried out with Whatman TLC glass plates (Partisil®K6F) pre-coated with silica gel  $60 \text{ \AA}$  with fluorescent indicator ( $\lambda = 254 \text{ nm}$ ). Gossypol was purchased from Funakoshi. All other chemicals were purchased from Wako Pure Chemicals Industries, Ltd., Kishida Chemicals Co., Ltd., GODO Co. Ltd., or Kanto Chemical Co., INC. and used without purification.

### 4.2. General synthetic protocol to access per-acetylated carbohydrates

To each of the commercially available carbohydrates (glucose, galactose, maltose, and lactose monohydrate), pyridine and acetic anhydride were added and the resultant heterogeneous mixture was stirred at the ambient temperature for several hours (see the following sections for details). After the mixture turned into transparent and TLC analyses on the mixture (toluene/ $\text{AcOEt} = 3/1$  v/v or  $1/1$  v/v) showed complete conversion of the substrate, the resultant mixture was diluted with ethyl acetate. We then added ice to the resultant organic solution and then, the organic layer was washed with  $0.5 \text{ N HCl aq}$  and  $\text{NaHCO}_3$ -saturated aqueous solutions, repeatedly. The organic layer was then dried over anhydrous  $\text{MgSO}_4$ , filtrated and evaporated to dryness to afford the corresponding per-acetylated carbohydrate as syrup or white powder.

#### 4.2.1. 1,2,3,4,6-Penta-O-acetyl-glucose (AcGlc, 1)

Glucose: 3.18 g; pyridine: 100 ml; acetic anhydride: 50 ml; reaction time: 17 h; yield: 87%; MALDI-TOF-MS:  $[\text{M}+\text{K}]^+ = 429.01$  (calc. 429.12).

#### 4.2.2. 1,2,3,4,6-Penta-O-acetyl-galactose (AcGal, 2)

Galactose: 4.52 g; pyridine: 100 ml; acetic anhydride: 50 ml; reaction time: 24 h; yield: 85%; MALDI-TOF-MS:  $[\text{M}+\text{Na}]^+ = 413.40$  (calc. 413.12).

Table 2  
 $IC_{50}$  estimated through the WST-8 assay.

	$IC_{50}/\mu\text{M}$		Relative HepG2-specificity <sup>a</sup>
	DLD-1	HepG2	
$\beta\text{Lac}_2\text{Gos}$	46	47	1.28
$\beta\text{Gal}_2\text{Gos}$	77	59	1.71
$\alpha\text{Gal}_2\text{Gos}$	13	>100	<0.17
$\beta\text{Mal}_2\text{Gos}$	33	42	1.03
$\alpha\text{Mal}_2\text{Gos}$	9	74	0.16
$\beta\text{Glc}_2\text{Gos}$	50	78	0.84
Gos	13	17	1.00

<sup>a</sup> Relative  $IC_{50}(\text{HepG2})/IC_{50}(\text{DLD-1})$  in comparison to that of Gos.

#### 4.2.3. 1,2,3,6,2',3',4',6'-Hexa-O-acetyl-maltose (AcMal, 3)

Maltose: 4.12 g; pyridine: 100 ml; acetic anhydride: 75 ml; reaction time: 43 h; yield: 97%; MALDI-TOF-MS:  $[M+Na]^+ = 701.46$  (calc. 701.20).

#### 4.2.4. 1,2,3,6,2',3',4',6'-Hexa-O-acetyl-lactose (AcLac, 4)

Lactose monohydrate: 10.02 g; pyridine: 200 ml; acetic anhydride: 100 ml; reaction time: 18 h; MALDI-TOF-MS:  $[M+Na]^+ = 701.54$  (calc. 701.20).

### 4.3. General synthetic protocol to access per-acetylated glycosyl bromides

To each of the per-acetylated carbohydrates (AcGlc, AcGal, AcMal, or AcLac) in  $CH_2Cl_2$ , acetic anhydride and 30% HBr in acetic acid were added and the resultant mixture was stirred at the ambient temperature for several hours. After TLC analysis of the mixture (toluene/AcOEt = 3/1 v/v or 1/1 v/v) showed complete consumption of the substrate, the resultant mixture was diluted with ethyl acetate. We then added ice to the resultant solution and then, the organic layer was washed with  $NaHCO_3$ -saturated aqueous solutions, repeatedly. The organic layer was dried over anhydrous  $MgSO_4$ , filtrated and evaporated to dryness to afford the corresponding bromide as syrup or white powder. The bromide was subjected to the subsequent glycosylation without any column purification processes.

#### 4.3.1. 1-[(2,3,4,6-Tetra-O-acetyl- $\beta$ -D-glucosyl)oxy]-2,5-pyrrolidinedione (AcGlcBr, 5)

AcGlc: 4.17 g;  $CH_2Cl_2$ : 50 ml; acetic anhydride: 4.0 ml; 30% HBr in acetic acid: 20 ml; reaction time: 1.5 h.

#### 4.3.2. 1-[(2,3,4,6-Tetra-O-acetyl- $\beta$ -D-galactosyl)oxy]-2,5-pyrrolidinedione (AcGalBr, 6)

AcGal: 4.00 g;  $CH_2Cl_2$ : 50 ml; acetic anhydride: 4.0 ml; 30% HBr in acetic acid: 18 ml; reaction time: 2.0 h.

#### 4.3.3. 1-[(2,3,6,2',3',4',6'-Hepta-O-acetyl- $\beta$ -maltosyl)oxy]-2,5-pyrrolidinedione (AcMalBr, 7)

AcMal: 3.48 g;  $CH_2Cl_2$ : 40 ml; acetic anhydride: 2.6 ml; 30% HBr in acetic acid: 12 ml; reaction time: 2.0 h.

#### 4.3.4. 1-[(2,3,6,2',3',4',6'-Hepta-O-acetyl- $\beta$ -lactosyl)oxy]-2,5-pyrrolidinedione (AcLacBr, 8)

AcLac: 4.13 g;  $CH_2Cl_2$ : 40 ml; acetic anhydride: 3.2 ml; 30% HBr in acetic acid: 15 ml; reaction time: 2.0 h.

### 4.4. General synthetic protocol to access per-acetylated carbohydrate derivatives having $\beta$ -linked NHS aglycon

To each of the bromides (AcGlcBr, AcGalBr, AcMalBr, or AcLacBr), NHS, TBAHS,  $CH_2Cl_2$  and 1 M  $Na_2CO_3$  aqueous solution were added, and the resultant heterogeneous solution was vigorously stirred at the ambient temperature. After TLC analysis (hexane/AcOEt = 1/4 v/v) of the mixture showed complete consumption of the substrate, the resultant mixture was diluted with ethyl acetate. We then washed the resultant organic layer with NaCl-saturated aqueous solutions, repeatedly. The organic layer was dried over anhydrous  $MgSO_4$ , filtrated and evaporated to dryness. The residue was subjected to silica-gel column purification (hexane/AcOEt = 10/0 to 0/10, gradient) to afford the titled compound.

#### 4.4.1. 1-[(2,3,4,6-Tetra-O-acetyl- $\beta$ -D-glucosyl)oxy]-2,5-pyrrolidinedione (AcGlc $\beta$ NHS, 9)

NHS: 5.30 g; TBAHS: 3.06 g;  $CH_2Cl_2$ : 70 ml;  $Na_2CO_3$  aq.: 70 ml;

reaction time: 13 h; yield: 35% (2 steps); white powder;  $R_f$  (hexane/AcOEt = 1/4) = 0.19;  $^1H$  NMR (300 MHz,  $CDCl_3$ ):  $\delta$  5.30–5.19 (m, 3H), 5.07 (d,  $J$  6.6 Hz, 1H), 4.30 (dd,  $J$  4.8, 12.6 Hz, 1H), 4.16 (dd,  $J$  3.0, 12.6 Hz, 1H), 3.77–3.69 (m, 1H), 2.74 (s, 4H), 2.13 (s, 3H), 2.09 (s, 3H), 2.03 (s, 6H);  $^{13}C$  NMR (75 MHz,  $CDCl_3$ ):  $\delta$  170.6, 170.1, 170.0, 169.4, 169.3, 103.8, 72.3, 72.2, 69.6, 68.1, 61.7, 25.4, 20.8, 20.7, 20.6, 20.6; MALDI-TOF-MS:  $[M+Na]^+ = 468.44$  (calc. 468.12); IR (KBr) 2965, 1755, 1738, 1380, 1278, 1227, 1188, 1076, 1032  $cm^{-1}$ .

#### 4.4.2. 1-[(2,3,4,6-Tetra-O-acetyl- $\beta$ -D-galactosyl)oxy]-2,5-pyrrolidinedione (AcGal $\beta$ NHS, 10)

NHS: 5.32 g; TBAHS: 3.06 g;  $CH_2Cl_2$ : 70 ml;  $Na_2CO_3$  aq.: 70 ml; reaction time: 10 h; yield: 56% (2 steps); white powder;  $R_f$  (hexane/AcOEt = 1/2) = 0.08;  $^1H$  NMR (300 MHz,  $CDCl_3$ ):  $\delta$  5.44–5.37 (m, 2H), 5.08 (dd,  $J$  4.8, 10.5 Hz, 1H), 4.92 (d,  $J$  8.1 Hz, 1H), 4.24 (dd,  $J$  6.3, 10.8 Hz, 1H), 4.15 (t,  $J$  7.5 Hz, 1H), 4.11 (dd,  $J$  7.2, 9.0 Hz, 1H), 3.92 (td,  $J$  0.9, 6.9 Hz, 1H), 2.75 (s, 4H), 2.18 (s, 3H), 2.15 (s, 3H), 2.04 (s, 3H), 2.01 (s, 3H);  $^{13}C$  NMR (75 MHz,  $CDCl_3$ ):  $\delta$  170.1, 170.0, 169.7, 169.5, 105.0, 70.9, 70.1, 66.6, 66.0, 60.4, 25.1, 20.5, 20.4, 20.4, 20.3; MALDI-TOF-MS:  $[M+Na]^+ = 468.44$  (calc. 468.12); IR (KBr) 2951, 1759, 1726, 1371, 1247, 1226, 1084  $cm^{-1}$ .

#### 4.4.3. 1-[(2,3,6,2',3',4',6'-Hepta-O-acetyl- $\beta$ -maltosyl)oxy]-2,5-pyrrolidinedione (AcMal $\beta$ NHS, 11)

NHS: 2.75 g; TBAHS: 1.67 g;  $CH_2Cl_2$ : 50 ml;  $Na_2CO_3$  aq.: 50 ml; reaction time: 12 h; yield: 40% (2 steps); white powder;  $R_f$  (hexane/AcOEt = 1/4) = 0.18;  $^1H$  NMR (300 MHz,  $CDCl_3$ ):  $\delta$  5.43 (d,  $J$  3.9 Hz, 1H), 5.37 (t,  $J$  9.9 Hz, 1H), 5.22 (dd,  $J$  6.9, 8.1 Hz, 1H), 5.17 (d,  $J$  6.6 Hz, 1H), 5.09 (t,  $J$  6.9 Hz, 1H), 5.05 (t,  $J$  9.9 Hz, 1H), 4.84 (dd,  $J$  4.2, 10.2 Hz, 1H), 4.45 (dd,  $J$  3.3, 12.0 Hz, 1H), 4.38–4.25 (m, 3H), 4.15–3.98 (m, 2H), 3.86–3.81 (m, 1H), 3.98 (s, 4H), 2.75 (s, 4H), 2.15 (s, 3H), 2.12 (s, 6H), 2.04 (s, 6H), 2.03 (s, 3H), 2.01 (s, 3H);  $^{13}C$  NMR (75 MHz,  $CDCl_3$ ):  $\delta$  170.4, 170.3, 170.2, 170.1, 169.8, 169.8, 169.2, 169.2, 102.2, 95.3, 74.7, 72.3, 72.2, 70.2, 69.9, 69.0, 68.3, 67.8, 62.5, 61.4, 25.2, 20.8, 20.6, 20.6, 20.5, 20.4, 20.4; MALDI-TOF-MS:  $[M+Na]^+ = 756.55$  (calc. 756.21); IR (KBr) 2961, 1748, 1433, 1371, 1234, 1038  $cm^{-1}$ .

#### 4.4.4. 1-[(2,3,6,2',3',4',6'-Hepta-O-acetyl- $\beta$ -lactosyl)oxy]-2,5-pyrrolidinedione (AcLac $\beta$ NHS, 12)

NHS: 3.32 g; TBAHS: 1.94 g;  $CH_2Cl_2$ : 50 ml;  $Na_2CO_3$  aq.: 50 ml; reaction time: 8.5 h; yield: 56% (2 steps); white powder;  $R_f$  (hexane/AcOEt = 1/4) = 0.19;  $^1H$  NMR (300 MHz,  $CDCl_3$ ):  $\delta$  5.35 (d,  $J$  2.1 Hz, 1H), 5.24–5.09 (m, 4H), 4.98 (dd,  $J$  3.3, 10.8 Hz, 1H), 4.56 (d,  $J$  8.1 Hz, 1H), 4.44 (dd,  $J$  1.8, 11.7 Hz, 1H), 4.23–4.05 (m, 4H), 3.90 (dd,  $J$  6.6, 7.2 Hz, 1H), 3.80–3.75 (m, 1H), 2.74 (s, 4H), 2.16 (s, 3H), 2.13 (s, 3H), 2.12 (s, 3H), 2.09 (s, 3H), 2.07 (s, 3H), 2.06 (s, 3H), 1.97 (s, 3H);  $^{13}C$  NMR (75 MHz,  $CDCl_3$ ):  $\delta$  170.3, 170.2, 170.1, 170.0, 169.5, 169.2, 169.1, 102.1, 101.1, 75.7, 72.8, 72.6, 70.8, 70.7, 69.9, 68.9, 66.6, 61.8, 60.8, 25.3, 20.8, 20.7, 20.6, 20.4; MALDI-TOF-MS:  $[M+Na]^+ = 756.49$  (calc. 756.21); IR (KBr) 2948, 1750, 1637, 1433, 1372, 1230, 1070  $cm^{-1}$ .

### 4.5. General synthetic protocol to access carbohydrate derivatives having O- $\beta$ -linked NHS aglycon

To each of the per-acetylated carbohydrates having NHS aglycon (AcGlc $\beta$ NHS, AcGal $\beta$ NHS, AcMal $\beta$ NHS, or AcLac $\beta$ NHS), dry MeOH and hydrazine monohydrate were added and the resultant mixture in tightly sealed flask was stirred for 3 min at the ambient temperature. We then took off the seal and kept the resultant mixture to be stirred for several hours under atmospheric conditions. White precipitate was gradually formed as the reaction proceeded. The resultant solution containing the white precipitate was again tightly sealed and kept at  $-69^\circ C$  overnight. The white precipitate was then filtered off and the filtrate was evaporated and dried in

vacuo. The resultant white powder was then re-dissolved into hot MeOH (ca. 60 °C), to which excess amount of CH<sub>2</sub>Cl<sub>2</sub> was added. The resultant white precipitate was retrieved from the mixture through filtration and then, purified on silica-gel (CH<sub>2</sub>Cl<sub>2</sub>/MeOH = 10/0 to 7/3 v/v, gradient). Note that the silica-gel was carefully washed with MeOH and dried before it was used in this column purification process. The titled compound was obtained as white powder.

#### 4.5.1. 1-O-Amino-β-D-glucopyranoside (GlcβONH<sub>2</sub>, 13)

AcGlcβNHS: 893 mg; dry MeOH: 20 ml; hydrazine monohydrate: 534 μl; reaction time: 3.3 h; yield: 17%; white powder; *R<sub>f</sub>* (CHCl<sub>3</sub>/MeOH/H<sub>2</sub>O = 4/5/1) = 0.49; <sup>1</sup>H NMR (300 MHz, D<sub>2</sub>O): δ 4.42 (d, 8.1 Hz, 1H), 3.78 (d, *J* 12.0 Hz, 1H), 3.58 (dd, *J* 6.0, 12.3 Hz, 1H), 3.39–3.30 (m, 2H), 3.23–3.12 (m, 2H); <sup>13</sup>C NMR (75 MHz, D<sub>2</sub>O): δ 105.6, 76.4, 72.2, 70.1, 61.3; IR (KBr) 3421, 3294, 2862, 1607, 1072 cm<sup>-1</sup>.

#### 4.5.2. 1-O-Amino-β-D-galactopyranoside (GalβONH<sub>2</sub>, 14)

AcGalβNHS: 895 mg; dry MeOH: 20 ml; hydrazine monohydrate: 534 μl; reaction time: 2.5 h; yield: 22%; white powder; *R<sub>f</sub>* (CHCl<sub>3</sub>/MeOH/H<sub>2</sub>O = 4/5/1) = 0.41; <sup>1</sup>H NMR (300 MHz, D<sub>2</sub>O): δ 4.37 (d, *J* 8.1 Hz, 1H), 3.77 (d, *J* 3.3 Hz, 1H), 3.70–3.56 (m, 3H), 3.52 (dd, *J* 3.3, 9.9 Hz, 1H), 3.37 (dd, *J* 8.4, 9.9 Hz, 1H); <sup>13</sup>C NMR (75 MHz, D<sub>2</sub>O): δ 106.1, 75.7, 73.4, 69.9, 69.2, 61.6; IR (KBr) 3348, 1432, 1184, 1146, 1075, 1033 cm<sup>-1</sup>.

#### 4.5.3. 1-O-Amino-β-maltoside (MalβONH<sub>2</sub>, 15)

AcMalβNHS: 732 mg; dry MeOH: 10 ml; hydrazine monohydrate: 468 μl; reaction time: 5.0 h; yield: 67%; white powder; *R<sub>f</sub>* (CHCl<sub>3</sub>/MeOH/H<sub>2</sub>O = 4/5/1) = 0.30; <sup>1</sup>H NMR (300 MHz, D<sub>2</sub>O): δ 5.24 (d, *J* 4.2 Hz, 1H), 4.42 (d, *J* 8.1 Hz, 1H), 3.81–3.45 (m, 9H), 3.49 (dd, *J* 3.6, 9.9 Hz, 1H), 3.27–3.14 (m, 2H); <sup>13</sup>C NMR (75 MHz, D<sub>2</sub>O): δ 105.6, 100.3, 77.4, 77.0, 75.2, 73.6, 73.5, 72.4, 72.3, 70.1, 61.5, 61.3; IR (KBr) 3531, 3307, 1160, 1056, 1028 cm<sup>-1</sup>.

#### 4.5.4. 1-O-Amino-β-lactoside (LacβONH<sub>2</sub>, 16)

AcLacβNHS: 733 mg; dry MeOH: 10 ml; hydrazine monohydrate: 468 μl; reaction time: 2.0 h; yield: 61%; white powder; *R<sub>f</sub>* (CHCl<sub>3</sub>/MeOH/H<sub>2</sub>O = 4/5/1) = 0.31; <sup>1</sup>H NMR (300 MHz, D<sub>2</sub>O): δ 4.43 (d, *J* 8.1 Hz, 1H), 4.27 (d, *J* 7.5 Hz, 1H), 3.83 (dd, *J* 1.8, 12.9 Hz, 1H), 3.75 (d, *J* 3.3 Hz, 1H), 3.68–3.45 (m, 8H), 3.37 (dd, *J* 7.5, 9.9 Hz, 1H), 3.23–3.13 (m, 1H); <sup>13</sup>C NMR (75 MHz, D<sub>2</sub>O): δ 105.4, 103.5, 78.7, 75.9, 75.3, 75.0, 73.0, 71.9, 71.5, 69.1, 61.6, 60.6; IR (KBr) 3366, 2890, 1622, 1077, 1056 cm<sup>-1</sup>.

#### 4.6. General synthetic protocol to access per-acetylated carbohydrate derivatives having O-α-linked NHS aglycon

To each of the per-acetylated carbohydrates (AcGal or AcMal), NHS, CH<sub>2</sub>Cl<sub>2</sub> and BF<sub>3</sub>OEt<sub>2</sub> were added, and the resultant mixture was stirred under N<sub>3</sub> at the ambient temperature. After complete consumption of the substrate was confirmed through TLC analysis (hexane/AcOEt = 2/1 v/v), precipitate that formed during the reaction was removed by filtration using Celite and the filtrate was diluted with ethyl acetate. The organic layer was then washed with NaHCO<sub>3</sub>-saturated aqueous solutions, repeatedly. The resultant organic layer was dried over anhydrous MgSO<sub>4</sub>, filtrated and evaporated to dryness. TLC analysis showed that the residue contained the titled compound along with some impurities containing the corresponding β-isomer (AcGalβNHS or AcMalβNHS). The residue was then subjected to silica-gel column purification (hexane/AcOEt = 10/0 to 1/2, gradient) to retrieve the titled compound in pure form. Since *R<sub>f</sub>* values of the titled compound and the corresponding β-isomer were so close to each other, this purification process greatly lowered the final yield. Especially, in the case of

AcMalβNHS, it is quite difficult to retrieve AcMalβNHS in pure form only through the silica-gel column purification process and the yield of the obtained AcMalβNHS was quite limited (7%). We therefore combined the fractions containing mixtures of AcMalβNHS and AcMalαNHS and the resultant solution was evaporated to dryness and then re-dissolved in AcOEt. Keeping the resultant AcMalβNHS/AcMalαNHS solution for several days in the ambient temperature gave AcMalβNHS as white precipitates (19%). Total yield was thus 26%.

#### 4.6.1. 1-[(2,3,4,6-Tetra-O-acetyl-α-D-galactosyl)oxy]-2,5-pyrrolidinedione (AcGalαNHS, 17)

AcGal: 5.53 g; NHS: 4.90 g; CH<sub>2</sub>Cl<sub>2</sub>: 38 ml; BF<sub>3</sub>OEt<sub>2</sub>: 8.9 ml; reaction time: 22 h; yield: 20%; white powder; *R<sub>f</sub>* (hexane/AcOEt = 1/2) = 0.31; <sup>1</sup>H NMR (300 MHz, CDCl<sub>3</sub>): δ 5.58 (dd, *J* 1.2, 3.3 Hz, 1H), 5.52 (d, *J* 3.9 Hz, 1H), 5.48 (dd, *J* 3.3, 11.4 Hz, 1H), 5.23 (dd, *J* 4.2, 11.1 Hz, 1H), 5.06 (td, *J* 0.6, 6.3 Hz, 1H), 4.25 (dd, *J* 6.0, 11.4 Hz, 1H), 3.95 (dd, 6.3, 10.8 Hz, 1H), 2.74 (s, 4H), 2.19 (s, 3H), 2.15 (s, 3H), 2.07 (s, 3H), 2.02 (s, 3H); <sup>13</sup>C NMR (75 MHz, CDCl<sub>3</sub>): δ 170.7, 170.4, 170.4, 170.0, 169.7, 101.2, 68.5, 67.7, 66.7, 66.5, 61.2, 25.3, 20.7, 20.6, 20.6, 20.6; IR (KBr) 2970, 1750, 1734, 1433, 1372, 1228, 1137, 1074 cm<sup>-1</sup>.

#### 4.6.2. 1-[(2,3,6,2',3',4',6'-Hepta-O-acetyl-α-maltosyl)oxy]-2,5-pyrrolidinedione (AcMalαNHS, 18)

AcMal: 10.63 g; NHS: 5.40 g; CH<sub>2</sub>Cl<sub>2</sub>: 50 ml; BF<sub>3</sub>OEt<sub>2</sub>: 10.0 ml; reaction time: 24 h; yield: 26%; white powder; *R<sub>f</sub>* (toluene/AcOEt = 1/1) = 0.30; <sup>1</sup>H NMR (300 MHz, CDCl<sub>3</sub>): δ 5.65 (dd, *J* 9.0, 10.2 Hz, 1H), 5.46 (d, *J* 3.6 Hz, 1H), 5.42–5.35 (m, 2H), 5.10 (t, *J* 9.6 Hz, 1H), 4.90–4.81 (m, 3H), 4.60 (dd, *J* 2.4, 12.6 Hz, 1H), 4.29–4.21 (m, 2H), 4.08–3.96 (m, 3H), 2.73 (s, 4H), 2.15 (s, 3H), 2.14 (s, 3H), 2.11 (s, 3H), 2.08 (s, 3H), 2.06 (s, 3H), 2.04 (s, 3H), 2.01 (s, 3H); <sup>13</sup>C NMR (75 MHz, CDCl<sub>3</sub>): δ 170.7, 170.6, 170.5, 170.3, 170.2, 169.8, 169.6, 169.5, 100.3, 95.6, 71.8, 71.0, 70.1, 70.0, 69.9, 69.3, 68.4, 67.8, 61.9, 61.2, 25.3, 20.9, 20.8, 20.7, 20.6, 20.6, 20.5; IR (KBr) 1748, 1434, 1371, 1235, 1038 cm<sup>-1</sup>.

#### 4.7. General synthetic protocol to access carbohydrate derivatives having O-α-linked NHS aglycon

To each of the per-acetylated carbohydrates having NHS aglycon (AcGalαNHS or AcMalαNHS), dry MeOH and hydrazine monohydrate were added and the resultant mixture in tightly sealed flask was stirred for 3 min at the ambient temperature. We then took off the seal and kept the resultant mixture to be stirred for 3 h under atmospheric conditions. White precipitate was gradually formed as the reaction proceeded. The resultant solution containing the white precipitate was again tightly sealed and kept at -57 °C for 13 h. The white precipitate was then filtered off and the filtrate was evaporated and dried in vacuo. The resultant white powder was then re-dissolved into hot MeOH (ca. 60 °C), to which excess amount of CH<sub>2</sub>Cl<sub>2</sub> was added. The resultant white precipitate was retrieved from the mixture through filtration and then, purified on silica-gel (CH<sub>2</sub>Cl<sub>2</sub>/MeOH = 10/0 to 7/3 v/v, gradient). Note that the silica-gel was carefully washed with MeOH and dried before it was used in this column purification process. The titled compound was obtained as white powder.

#### 4.7.1. 1-O-Amino-α-D-galactoside (GalαONH<sub>2</sub>, 19)

AcGalαNHS: 446 mg; hydrazine: 267 μl; dry MeOH: 10 ml; reaction time: 3 h; yield: 27%; white powder; *R<sub>f</sub>* (CH<sub>2</sub>Cl<sub>2</sub>/MeOH = 7/3) = 0.67; <sup>1</sup>H NMR (300 MHz, D<sub>2</sub>O): δ 4.86 (d, *J* 3.9 Hz, 1H), 3.82–3.75 (m, 2H), 3.69 (dd, *J* 3.9, 10.5 Hz, 1H), 3.64–3.54 (m, 3H); <sup>13</sup>C NMR (75 MHz, D<sub>2</sub>O): δ 102.4, 71.5, 69.8, 69.7, 68.4, 61.6; IR (KBr) 3431, 2538, 1602, 1457, 1417, 1353, 1227, 1133, 1074 cm<sup>-1</sup>.

#### 4.7.2. 1-O-Amino- $\alpha$ -maltoside (Mal $\alpha$ ONH<sub>2</sub>, 20)

AcMal $\alpha$ NHS: 367 mg; hydrazine: 234  $\mu$ l; dry MeOH: 5 ml; reaction time: 3 h; yield: 50%; white powder;  $R_f$  (CHCl<sub>3</sub>/MeOH/H<sub>2</sub>O = 4/5/1) = 0.30; <sup>1</sup>H NMR (300 MHz, D<sub>2</sub>O):  $\delta$  5.21 (d, *J* 3.6 Hz, 1H), 4.81 (d, *J* 4.2 Hz, 1H), 3.74–3.36 (m, 11H), 3.23 (t, *J* 9.6 Hz, 1H); <sup>13</sup>C NMR (75 MHz, D<sub>2</sub>O):  $\delta$  101.8, 100.0, 77.0, 73.7, 73.3, 73.1, 72.1, 71.1, 70.7, 69.7, 60.9, 60.7.

#### 4.8. General synthetic protocol to access Gos having two carbohydrate appendages

Each of the 1-O-amino-carbohydrates (3 eq.) was added to Gos (1 eq.) in dry MeOH, and the resultant solution was stirred for several hours. The resultant solution was evaporated to dryness followed by dissolution with dry MeOH. This evaporation-dissolution process was repeated for several times. After TLC analysis (CHCl<sub>3</sub>/MeOH/H<sub>2</sub>O = 4/5/1, v/v/v) of the resultant solution showed complete conversion from Gos to the desired product having two carbohydrate-appendages, limited amount of water was added. The water-insoluble compound (the glycoGos) was retrieved by filtration followed by drying in vacuo to give the titled compound. Note that the glycoGos were slightly water-soluble so that certain amounts of the glycoGos were dissolved into the filtrates. We assume that the partial dissolution of the glycoGos into the filtrates should be responsible for the deteriorated yields in this synthetic step. This assumption was paradoxically supported by the fact that  $\beta$ Glc<sub>2</sub>Gos that is the least water-soluble glycoGos in this study was obtained in the highest yield (99%). In this case, the hardly water-soluble nature of  $\beta$ Glc<sub>2</sub>Gos should minimize the lost of  $\beta$ Glc<sub>2</sub>Gos into the filtrate to improve the recovery efficiency.

##### 4.8.1. $\beta$ Glc<sub>2</sub>Gos (21)

Glc $\beta$ ONH<sub>2</sub>: 28 mg; Gos: 32 mg; dry MeOH: 5 ml; reaction time: 4 h; yield: 99%; pale yellow powder;  $R_f$  (CHCl<sub>3</sub>/MeOH/H<sub>2</sub>O = 4/5/1) = 0.76; <sup>1</sup>H NMR (300 MHz, CD<sub>3</sub>OD):  $\delta$  10.03 (br s, 2H), 7.67 (br s, 2H), 5.03 (d, *J* 6.3 Hz, 2H), 3.89 (dd, *J* 2.1, 9.3 Hz, 2H), 3.71 (dd, *J* 4.5, 12 Hz, 2H), 3.49–3.29 (m), 2.04 (s), 1.55–1.52 (m); <sup>13</sup>C NMR (75 MHz, CD<sub>3</sub>OD):  $\delta$  157.8, 152.2, 149.1, 145.3, 134.5, 131.3, 129.7, 118.0, 117.1, 107.0, 106.1, 78.3, 78.2, 73.6, 71.2, 62.5, 30.7, 20.9, 20.7; ESI-TOF-MS: [M+H]<sup>+</sup> = 873.4611 (calc. 873.3293 for C<sub>42</sub>H<sub>53</sub>N<sub>2</sub>O<sub>18</sub>); IR (KBr) 3399, 2926, 1616, 1424, 1323, 1244, 1179, 1075 cm<sup>-1</sup>.

##### 4.8.2. $\beta$ Gal<sub>2</sub>Gos (22)

Gal $\beta$ ONH<sub>2</sub>: 27 mg; Gos: 36 mg; dry MeOH: 5 ml; reaction time: 4 h; yield: 48%; pale yellow powder;  $R_f$  (CHCl<sub>3</sub>/MeOH/H<sub>2</sub>O = 4/5/1) = 0.70; <sup>1</sup>H NMR (300 MHz, CD<sub>3</sub>OD):  $\delta$  10.03 (s, 2H), 7.69 (s, 2H), 5.01 (d, *J* 8.1 Hz, 2H), 3.95 (br s, 2H), 3.89 (d, *J* 4.5 Hz, 2H), 3.81–3.62 (m, 8H), 3.57 (dd, *J* 3.3, 9.6 Hz, 2H), 2.04 (s, 4H), 1.55–1.51 (m, 12H); <sup>13</sup>C NMR (75 MHz, CD<sub>3</sub>OD):  $\delta$  157.7, 152.3, 149.0, 145.2, 134.5, 131.3, 129.7, 118.0, 117.6, 117.1, 107.0, 106.7, 77.0, 75.1, 71.0, 70.2, 62.4, 35.0, 33.1, 30.7, 30.4, 30.2, 28.6, 26.1, 23.7, 20.9, 20.7, 14.2; ESI-TOF-MS: [M+H]<sup>+</sup> = 873.4482 (calc. 873.3293 for C<sub>42</sub>H<sub>53</sub>N<sub>2</sub>O<sub>18</sub>); IR (KBr) 3421, 2926, 1618, 1424, 1323, 1078 cm<sup>-1</sup>.

##### 4.8.3. $\beta$ Mal<sub>2</sub>Gos (23)

Mal $\beta$ ONH<sub>2</sub>: 55 mg; Gos: 40 mg; dry MeOH: 5 ml; reaction time: 4.5 h; yield: 42%; pale yellow powder;  $R_f$  (CHCl<sub>3</sub>/MeOH/H<sub>2</sub>O = 4/5/1) = 0.54; <sup>1</sup>H NMR (300 MHz, DMF-*d*<sub>7</sub>):  $\delta$  11.85 (br s, 2H), 10.15 (s, 2H), 8.94 (br s, 2H), 7.71 (s, 2H), 5.76–1.53 (m); <sup>13</sup>C NMR (75 MHz, DMF-*d*<sub>7</sub>):  $\delta$  155.4, 150.9, 147.4, 143.4, 139.2, 132.7, 128.9, 127.6, 117.6, 115.5, 105.2, 104.3, 100.9, 79.1, 76.2, 75.4, 73.3, 72.6, 71.6, 70.1, 61.0, 60.2, 19.5, 19.3; ESI-TOF-MS: [M+H]<sup>+</sup> = 1197.4374 (calc. 1197.4350 for C<sub>54</sub>H<sub>73</sub>N<sub>2</sub>O<sub>28</sub>); IR (KBr) 3389, 2928, 1631, 1424, 1323, 1244, 1146, 1071, 1047 cm<sup>-1</sup>.

##### 4.8.4. $\beta$ Lac<sub>2</sub>Gos (24)

Lac $\beta$ ONH<sub>2</sub>: 185 mg; Gos: 82 mg; dry MeOH: 5 ml; reaction time: 5 h; yield: 31%; pale yellow powder;  $R_f$  (CHCl<sub>3</sub>/MeOH/H<sub>2</sub>O = 4/5/1) = 0.64; <sup>1</sup>H NMR (300 MHz, DMF-*d*<sub>7</sub>):  $\delta$  11.84 (br s, 2H), 10.15 (s, 2H), 8.93 (br s, 2H), 7.71 (s, 2H), 5.63–1.52 (m); <sup>13</sup>C NMR (75 MHz, DMF-*d*<sub>7</sub>):  $\delta$  155.4, 150.9, 147.4, 132.7, 128.9, 127.6, 117.5, 115.5, 105.2, 104.1, 103.8, 80.3, 75.4, 74.9, 73.3, 71.7, 70.7, 68.2, 60.5, 19.5, 19.3; ESI-TOF-MS: [M+H]<sup>+</sup> = 1197.4374 (calc. 1197.4350 for C<sub>54</sub>H<sub>73</sub>N<sub>2</sub>O<sub>28</sub>); IR (KBr) 3390, 2926, 1633, 1424, 1323, 1072 cm<sup>-1</sup>.

##### 4.8.5. $\alpha$ Gal<sub>2</sub>Gos (25)

Gal $\alpha$ ONH<sub>2</sub>: 104 mg; Gos: 50 mg; dry MeOH: 2 ml; reaction time: 3.0 h; yield: 27%; pale yellow powder;  $R_f$  (CHCl<sub>3</sub>/MeOH = 2/1) = 0.32; <sup>1</sup>H NMR (300 MHz, CD<sub>3</sub>OD):  $\delta$  10.03 (br s, 2H), 7.69 (br s, 2H), 5.56 (d, *J* 4.2 Hz, 2H), 4.00–3.58 (m), 3.31 (m), 2.04 (s), 1.55–1.51 (m); <sup>13</sup>C NMR (75 MHz, CD<sub>3</sub>OD):  $\delta$  158.2, 158.1, 152.1, 149.1, 145.3, 134.5, 133.6, 131.2, 129.6, 117.9, 117.9, 117.6, 117.0, 107.0, 102.8, 72.9, 71.3, 70.7, 69.5, 62.3, 30.7, 28.5, 28.4, 20.9; ESI-TOF-MS: [M+H]<sup>+</sup> = 873.3293 (calc. 873.3293 for C<sub>42</sub>H<sub>53</sub>N<sub>2</sub>O<sub>18</sub>); IR (KBr) 3398, 2931, 1635, 1427, 1319, 1080 cm<sup>-1</sup>.

##### 4.8.6. $\alpha$ Mal<sub>2</sub>Gos (26)

Mal $\alpha$ ONH<sub>2</sub>: 91 mg; Gos: 15 mg; dry MeOH: 2 ml; reaction time: 3.0 h; yield: 50%; pale yellow powder;  $R_f$  (CHCl<sub>3</sub>/MeOH/H<sub>2</sub>O = 4/5/1) = 0.59; <sup>1</sup>H NMR (300 MHz, CD<sub>3</sub>OD):  $\delta$  10.07–10.04 (m, 2H), 7.69 (s, 2H), 5.55–5.54 (m, 2H), 5.19–6.16 (m, 2H), 3.99–3.20 (m), 2.17–2.03 (m), 1.55–1.52 (m); <sup>13</sup>C NMR (75 MHz, CD<sub>3</sub>OD):  $\delta$  158.3, 158.3, 152.2, 152.1, 149.1, 149.0, 145.2, 134.5, 131.3, 129.7, 118.0, 118.0, 117.6, 117.0, 107.0, 107.0, 102.8, 102.8, 102.4, 102.3, 81.2, 81.1, 75.0, 74.9, 74.8, 74.7, 74.7, 74.2, 74.1, 72.9, 72.9, 72.4, 71.4, 71.4, 62.7, 61.7, 61.7, 58.3, 20.9, 20.8, 20.8, 18.4; ESI-TOF-MS: [M+H]<sup>+</sup> = 1197.5671 (calc. 1197.4350 for C<sub>54</sub>H<sub>73</sub>N<sub>2</sub>O<sub>28</sub>); IR (KBr) 3389, 2927, 1617, 1426, 1320, 1035 cm<sup>-1</sup>.

#### 4.9. WST-8 assays

Cell viability upon the glycoGos administration was assessed through a well-known protocol using a Cell Counting Kit-8 (Dojindo Molecular Technologies, Inc.). Briefly, 100  $\mu$ l of DLD-1 and HepG2 cell suspensions (30000 cells/ml) were incubated in 96-well plates at 37 °C with RPMI 1640 culture media, or 10% fetal bovine serum (FBS) containing 0.5% penicillin streptomycin, for 24 h in a CO<sub>2</sub> incubator. After the incubation, the media was removed from the wells using an aspirator and then, 100  $\mu$ l of RPMI 1640 media containing 0.2% DMF and varying concentration of the glycoGos were applied to the wells. After 48 h incubation, 10  $\mu$ l of Cell Counting Kit-8 solution were applied to the wells, and cells were further incubated at 37 °C for 30 min in the CO<sub>2</sub> incubator. Color development was monitored at 450 nm with a multi-well plate reader (SUNRISE Rainbow RC-R, Tecan) in which absorbance at 650 nm was used as a reference.

#### 4.10. Trypan blue exclusion test

DLD-1 and HepG2 cell suspensions (3 ml, 30000 cells/ml) were incubated on culture dishes for 24 h at 37 °C with RPMI 1640 culture media (10% FBS containing 0.5% penicillin streptomycin) for 24 h. After the incubation, the media were removed from the plates using an aspirator and then, 3 ml of the glycoGos solutions (RPMI 1640 media containing 2% FBS, 0.2% DMF and varying concentration of the glycoGos or Gos) were applied to the plates. After 48 h incubation of the cells at 37 °C, the supernatants were retrieved from the culture dishes (supernatant-1). The dishes with DLD-1 or HepG2 cells were then added with FBS and then, the supernatants were again retrieved from the culture dishes (supernatant-2). The

DLD-1 and HepG2 cells on the culture dishes were washed with PBS. Trypsin-EDTA solution was added to the dishes those were then incubated for 5 min. The resultant media containing DLD-1 or HepG2 cells were retrieved and then mixed with the supernatants (supernatant-1 and -2) in 15 ml centrifuge tube. The DLD-1 or HepG2 cells were collected through the centrifugation and re-suspended with RPMI 1640 media. The resultant cell suspensions were mixed with the equal volumes of trypan blue solution to be observed by using an optical micrometer Primo Vert, Zeiss).

### Acknowledgement

This research was partially supported by Special Research Fund of Toyo University.

### Appendix A. Supplementary data

Supplementary data associated with this article (structures of the representative Gos isomers with interconversions, chemical structures of  $\alpha$ Mal<sub>2</sub>Gos<sub>ii</sub>,  $\alpha$ Mal<sub>2</sub>Gos<sub>ei</sub>, and  $\alpha$ Mal<sub>2</sub>Gos<sub>ee</sub> for the MD calculations, plots of the potential energies during the dynamics, colored version of Fig. 2-(a), microscopic image of the HepG2 cells after the  $\beta$ Gal<sub>2</sub>Gos-treatment followed by trypan blue staining, and <sup>1</sup>H/<sup>13</sup>C NMR spectra of the synthetic compounds) can be found at <https://doi.org/10.1016/j.carres.2018.02.001>.

### References

- [1] M. Ionov, N.V. Gordiyenko, I. Zukowska, E. Tokhtaeva, O.A. Mareninova, N. Baram, K. Ziyaev, K. Rezhopov, M. Zamaraeva, *Int. J. Biol. Macromol.* 51 (2012) 908–914.
- [2] K. Dodou, R.J. Anderson, W.J. Lough, D.A.P. Small, M.D. Shelley, P.W. Groundwater, *Bioorg. Med. Chem.* 13 (2005) 4228–4237.
- [3] P. Przybylski, K. Pyta, J. Stefańska, M. Ratajczak-Sitarz, A. Katrusiak, A. Huczyński, B. Brzezinski, *Eur. J. Med. Chem.* 44 (2009) 4393–4403.
- [4] L. Li, Z. Li, K. Wang, Y. Liu, Y. Li, Q. Wang, *Bioorg. Med. Chem.* 24 (2016) 474–483.
- [5] S.Z.A. Badawy, A. Souid, V. Cuenca, N. Montalto, F. Shue, *Asian J. Androl.* 9 (2007) 388–393.
- [6] L. Huang, J. Hu, W. Tao, Y. Li, G. Li, P. Xie, X. Liu, J. Jiang, *Eur. J. Pharmacol.* 645 (2010) 9–13.
- [7] X. Wang, J. Wang, S.C.H. Wong, L.S.N. Chow, J.M. Nicholls, Y.C. Wong, Y. Liu, D.L.W. Kwong, J.S.T. Sham, S.W. Tsao, *Life Sci.* 67 (2000) 2663–2671.
- [8] C.V. Poznak, A.D. Seidman, M.M. Reidenberg, M.M. Moasser, N. Sklarin, K.V. Zee, P. Borgen, M. Gollub, D. Bacotti, T. Yao, R. Bloch, M. Ligueros, M. Sonenberg, L. Norton, C. Hudis, *Breast Canc. Res. Treat.* 66 (2001) 239–248.
- [9] J. Yang, F. Zhang, J. Li, G. Chen, S. Wu, W. Ouyang, W. Pan, R. Yu, J. Yang, P. Tien, *Bioorg. Med. Chem. Lett* 22 (2012) 1415–1420.
- [10] J. Yang, G. Chen, L.L. Li, W. Pan, F. Zhang, J. Yang, S. Wu, P. Tien, *Bioorg. Med. Chem. Lett* 23 (2013) 2619–2623.
- [11] N.I. Baram, A.I. Ismailov, K.L. Ziyaev, K.Z. Rezhopov, *Chem. Nat. Compd.* 40 (2004) 199–205.
- [12] V. Dao, C. Gaspard, M. Mayer, G.H. Werner, S.N. Nguyen, R.J. Michelot, *Eur. J. Med. Chem.* 35 (2000) 805–813.
- [13] L. Li, Z. Li, K. Wang, S. Zhao, J. Feng, J. Li, P. Yang, Y. Liu, L. Wang, Y. Li, H. Shang, Q. Wang, *Design, J. Agric. Food Chem.* 62 (2014) 11080–11088.
- [14] J. Yang, F. Zhang, J. Li, G. Chen, S. Wu, W. Ouyang, W. Pan, R. Yu, J. Yang, P. Tien, *Bioorg. Med. Chem. Lett* 22 (2012) 1415–1420.
- [15] V. Dao, M.K. Dowd, M.T. Martin, C. Gaspard, M. Mayer, R.J. Michelot, *Eur. J. Med. Chem.* 39 (2004) 619–624.
- [16] J. Yang, J. Li, J. Yang, L. Li, W. Ouyang, S. Wu, F. Zhang, *Chin. Chem. Lett.* 25 (2014) 1052–1056.
- [17] J. Yin, L. Jin, F. Chen, X. Wang, A. Kitaygorodskiy, Y. Jiang, *Carbohydr. Res.* 346 (2011) 2070–2074.
- [18] J. Zhang, J. Lv, X. Wang, D. Li, Z. Wang, G. Li, *Nano Res.* 8 (2015) 3853–3863.
- [19] K.D. McReynolds, D. Dimas, H. Le, *Tetrahedron Lett.* 55 (2014) 2270–2273.
- [20] P.K. Dhal, S.C. Polomoscanik, D.A. Gianolio, P.G. Starremans, M. Busch, K. Alving, B. Chen, R.J. Miller, *Bioconjugate Chem.* 24 (2013) 865–877.
- [21] C. Pifferi, G.C. Daskhan, M. Fiore, T.C. Shiao, R. Roy, O. Renaudet, *Chem. Rev.* 117 (2017) 9839–9873.
- [22] T.C. Shiao, A. Papadopoulos, O. Renaudet, R. Roy, Preparation of O- $\beta$ -D-galactopyranosyl-hydroxylamine, in: P. Kováč (Ed.), *Carbohydrate Chemistry: Proven Synthetic Methods*, vol. 1, CRC Press, 2012, pp. 289–293.
- [23] Y. Nonaka, R. Uruno, F. Dai, R. Matsuoka, M. Nakamura, M. Iwamura, H. Iwabuchi, T. Okada, N. Chigira, Y. Amano, T. Hasegawa, *Tetrahedron* 72 (2016) 5456–5464.
- [24] F. Yan, X. Cao, H. Jiang, X. Zhao, J. Wang, Y. Lin, Q. Liu, C. Zhang, B. Jiang, F. Guo, *J. Med. Chem.* 53 (2010) 5502–5510.
- [25] K. Sadahira, M. Sagawa, T. Nakazato, H. Uchida, Y. Ikeda, S. Okamoto, H. Nakajima, M. Kizaki, *Int. J. Oncol.* 45 (2014) 2278–2286.